Mechanism of H−H Activation by Nickel−Iron Hydrogenase

ARTICLE *in* JOURNAL OF THE AMERICAN CHEMICAL SOCIETY · JANUARY 1998

Impact Factor: 12.11 · DOI: 10.1021/ja971681+

Mechanism of H−H Activation by Nickel−Iron Hydrogenase

Maria Pavlov,*,† Per E. M. Siegbahn,*,† Margareta R. A. Blomberg,† and Robert H. Crabtree‡

Contribution from the Department of Physics, Stockholm University, Box 6730, S-113 85 Stockholm, Sweden, and Chemistry Department, Yale University, 225 Prospect Street, New Haven, Connecticut, 06520-8107

Received May 22, 1997. Revised Manuscript Received October 1, 1997

Abstract: DFT quantum chemical methods are used to probe the mechanism of the nickel−iron hydrogenases. Starting from the experimental X-ray structure, all plausible oxidation states and spin states were investigated. The structure and reactivity pattern of the NiFe cluster are best reproduced by assuming a NiFe(II,III) oxidation state assignment of the resting state of the cluster. In our proposed mechanism of H_2 oxidation by the enzyme, H_2 first binds to Fe in the form of a molecular hydrogen complex, which then undergoes heterolytic splitting. This process is spin-dependent and does not occur for the high-spin sextet state. In the key step, hydride transfer to iron and proton transfer to the adjacent cysteinethiolate ligand is accompanied by decoordination of the protonated cysteinethiol from Ni while remaining bound to iron. Simultaneously, the cyanide ligand on iron binds with the nickel atom in a rare bridging binding mode. After the H_2 dissociation, the hydride bound to Fe can then be transferred to Ni which should be a necessary preliminary for subsequent hydrogen atom or electron transport. The transition state for hydrogen splitting was located, and the resulting calculated energy barrier is in remarkably good agreement with the experimental value.

I. Introduction

The hydrogenase enzymes,[1] which catalyze the interconversion of dihydrogen and protons (eq 1), allow the use of H_2 as an energy source or the disposal of excess electrons in the form of H_2. In one physiological role,[2] H_2 crosses the bacterial

$$H_2 \Leftrightarrow 2H^+ + 2e^- \quad (1)$$

membrane and undergoes the oxidation reaction of eq 1. The resulting transmembrane pH gradient drives ATP formation via ATPase. A typical fate of the electrons also formed in eq 1 is acetyl-CoA synthesis. Hydrogenases from the sulfate-reducing bacterium, *Desulfovibrio gigas*, the photosynthetic bacterium, *Chromatium vinosum*, and the H_2-oxidizing bacterium, *Alcaligenes eutrophus*, among others, have been studied in detail. Hydrogenases also recapture the reducing power lost in nitrogen fixation by the unavoidable formation of H_2 as a byproduct in N_2 reduction by nitrogenase.

Four main classes of hydrogenases are recognized: the nickel−iron hydrogenases contain both metals and are the most numerous, followed by the Ni−Fe−Se enzymes which also contain one selenocysteine residue as a ligand for Ni. Fe-only enzymes are also known and strong evidence for the existence of a fourth class, a novel metal-free hydrogenase, has recently been gathered by Thauer et al.[3] The presence of essential nickel in the Ni−Fe enzymes, recognized since 1981,[4] attracted attention because Ni only rarely takes on this role in biology.[5] Depending on the source, nickel−iron hydrogenases contain different numbers of metal clusters, but there appears always to be at least one Ni-containing cluster and at least one Fe−S cluster. The former is usually considered as the site of H_2 binding and the latter as being involved in electron transfer. Many hydrogenases also contain additional Fe−S clusters or a more complex subunit structure; some are soluble, and others are membrane-bound.[5]

In a major step forward, the X-ray crystal structure of the iron−nickel hydrogenase from *D. gigas* was recently solved, albeit for the inactive air-oxidized form.[6a] The larger of the two subunits (60 kDa) contains a cluster having a nickel and another metal, at first only tentatively but later definitively identified as iron.[6b] The smaller 28 kDa subunit contains the Fe−S clusters. The Ni−Fe cluster consists of a Ni bound to four cysteinethiolates, two of which are of bridging mode with the Fe atom. An additional bridge between Fe and Ni is tentatively identified as a μ-oxo or -hydroxo group and considered to be associated with the oxidized inactive form of the enzyme, reduction to give the active form being accompanied by loss of this group. The asymmetry of the bridge (Ni−O, 1.7 Å; Fe−O, 2.1 Å) has led to the suggestion that a Ni═O → Fe bridge is present. The iron contains three terminal ligands that do not seem to be derived from the polypeptide but have the electron density appropriate for a two-atom ligand, such as CO.

In more recent infrared spectroscopic work on the *C. vinosum*[7] and *D. gigas*[6b] enzymes, three bands were detected in the 1900−2100 cm^{-1} range and considered to arise from CO, CN, or NO. Isotope studies identify the diatomic ligand set as $Fe(CN)_2(CO)$.[8]

† Stockholm University.
‡ Yale University.

(1) Albracht, S. P. J. *Biochim. Biophys. Acta* **1994**, *1188*, 167−204.
(2) Collman, J. P. *Nature Struct. Biol*. **1996**, *3*, 213.
(3) Thauer, R. K.; Klein, A. R.; Hartmann, G. C. *Chem. Rev*. **1996**, *96*, 3031−42.
(4) Graf, E. G.; Thauer, R. K. *FEBS Lett.* **1981**, *136*, 165.
(5) *The Bioinorganic Chemistry of Nickel*; Lancaster, J. R., Ed.; VCH: Weinheim, 1988.
(6) (a) Volbeda, A.; Charon, M. H.; Piras, C.; Hatchikian, E. C.; Frey, M.; Fontecilla-Camps, J. C. *Nature* **1995**, *373*, 580−7. (b) Volbeda, A.; Garcin, E.; Piras, C.; de Lacey, A. L.; Fernandez, V. M.; Hatchikian, E. C.; Frey, M.; Fontecilla-Camps, J. C. *J. Am. Chem. Soc*. **1996**, *118*, 12989−96.
(7) Bagley, K. A.; Duin, E. C.; Roseboom, W.; Albracht, S. P. J.; Woodruff, W. H. *Biochemistry* **1995**, *34*, 5527−35.

S0002-7863(97)01681-8 CCC: $15.00
Published on Web 01/13/1998

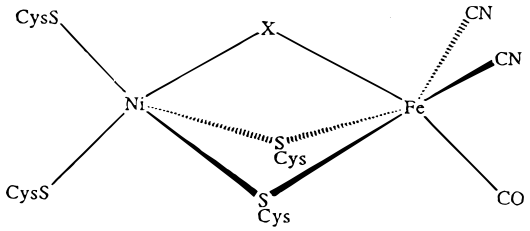

Figure 1. A schematic diagram of the active site of *D. gigas* hydrogenase from X-ray data[6] and IR data.[8] In the oxidized isolated form of the enzyme, X may be O, but this group is assumed to be removed by the reductive activation process.

The resulting structure for the Ni−Fe cluster of the *D. gigas* protein is shown in Figure 1.

The EPR data for *D. gigas* H_2-ase[9a] indicates the accessibility of several different enzyme states. Under aerobic conditions, an inactive form is isolated which can show two types of EPR signals, known as Ni-A (unready form) and Ni-B (ready form), as well as an EPR-silent form. The ready form can be rapidly activated by H_2 in the presence of certain electron carriers, to give the active form that shows the Ni-C EPR signal; reduction and oxidation of this form yield two further EPR-silent forms. The Ni-A form is only activated by H_2 over several hours. The Ni-C form is sensitive to visible light, and below 100 K a change in the EPR signal to Ni-C′ is seen on irradiation. This photoreaction shows a strong kinetic isotope effect (k_H/k_D = 6). CO is a competitive inhibitor with H_2, and photolysis of the CO-inhibited form also gives the Ni-C′ signal. The Ni-A, -B, and -C signals all show significant hyperfine coupling to ^{61}Ni, so they must be associated with the Ni−Fe cluster. These results suggest that the Ni−Fe cluster is the active site where CO and H_2 both interact.

At one time the EPR spectra were generally considered to indicate that the Ni ion itself is redox-active and able to attain different oxidation states, such as Ni(III) and Ni(I). This idea has been challenged because the Ni X-ray absorption edge shows no shift between the Ni-A, Ni-B, and Ni-C states, both for *D. gigas*[10] and *Thiocapsa roseopersicina* enzymes.[11] Additionally, no model compounds show Ni(I)/(II) and Ni(II)/(III) redox potentials as closely spaced as a few hundred millivolts found in the enzyme.[12a,b] A number of interesting functional modeling studies have also been carried out.[12c−e]

Many mechanistic schemes have been proposed,[9a,b] but there is still no general agreement about the details. In this paper, we use quantum chemical methods in the hope of clarifying the situation. The use of high-accuracy quantum chemical methods in the field of biochemistry involving transition metals is very new. In general, for standard ab initio methods the systems are simply too big. Density functional theory (DFT) methods have for some time had the capacity of treating large enough systems, but the accuracy has been questionable. Recent work in this area,[13] incorporating gradient corrections of the density and Hartree−Fock exchange in a scheme parametrized against experiments has changed the situation dramatically. The accuracy of these types of hybrid methods is now almost of the same level as that obtained by the most advanced ab initio methods obtainable for small systems.[14] The use of empirical parameters has not had any significant effect on the range of applicability of these methods. Since only a few (in the present case three) parameters selected on physical grounds are used, the methods are equally applicable for systems for which the parameters have not been fitted, such as for transition metal complexes.[15] This is unlike the situation for the previous type of semiempirical schemes where many more parameters were used. The present DFT methods have previously been proven useful for biochemical systems. In an application to the mechanism of methane activation by methane monooxygenase (MMO), an unusual distorted structure was predicted for the key active complex denoted compound **Q**,[16] which later proved to be identical with the model suggested on the basis of recent EXAFS measurements.[17] The energetics obtained for the methane reaction is also in very good agreement with available experimental information. Exactly the same type of methods and procedures were used in the MMO study as in the present study of nickel−iron hydrogenase.

II. Computational Details

The calculations were performed in two steps. First, an optimization of the geometry was performed using the B3LYP method.[13] Double-ζ basis sets were used in this step. In the second step the energy was evaluated for the optimized geometry using very large basis sets including diffuse functions and with two polarization functions on each atom. The final energy evaluation was also performed at the B3LYP level. All the calculations were carried out using the GAUSSIAN-94 program.[18]

The B3LYP functional can be written as,[13,19]

$$F^{\mathrm{B3LYP}} = (1-A)F_x^{\mathrm{Slater}} + AF_x^{\mathrm{HF}} + BF_x^{\mathrm{Becke}} + CF_c^{\mathrm{LYP}} + (1-C)F_c^{\mathrm{VWN}}$$

where F_x^{Slater} is the Slater exchange, F_x^{HF} is the Hartree−Fock exchange, F_x^{Becke} is the gradient part of the exchange functional of Becke,[13] F_c^{LYP} is the correlation functional of Lee, Yang, and Parr,[20] and F_c^{VWN} is the correlation functional of Vosko, Wilk, and Nusair.[21] *A*, *B*, and *C* are the coefficients determined by Becke[13] using a fit to experimental heats of formation. However, it should be noted that Becke did not use F_c^{VWN} and F_c^{LYP} in the expression above when the

(8) (a) Cammack, R.; Fernandez, V. M.; Schneider, K. In ref 5, pp 167−190. (b) Moura, J. J. G.; Teixeira, M.; Moura, I.; LeGall, J. In ref 5, pp 191−224.

(9) Happe, R. P.; Roseboom, W.; Pierik, A. J.; Albracht, S. P. J.; Bagley, K. A. *Nature* **1997**, *385*, 126.

(10) Eidsness, M. K.; Sullivan, R. J.; Scott, R. A. In ref 5, pp 83−85.

(11) Bagyinka, C.; Whitehead, J. P.; Maroney, M. J. *J. Am. Chem. Soc.* **1993**, *115*, 3576−85.

(12) (a) Coyle, C. L.; Stiefel, E. I. In ref 5, pp 1−28. (b) Margerum, D. W.; Anliker, S. L. In ref 5, pp 29−50. (c) Hembre, R. T.; McQueen, J. S.; Day, V. W. *J. Am. Chem. Soc.* **1996**, *118*, 798−803. (d) Efros, L. E.; Thorp, H. H.; Brudvig, G. W.; Crabtree, R. H. *Inorg. Chem.* **1992**, *31*, 1722−4. (e) Beley, M.; Collin, J.-P.; Ruppert, R.; Sauvage, J.-P. *J. Am. Chem. Soc.* **1986**, *108*, 7461.

(13) Becke, A. D. *Phys. Rev.* **1988**, *A38*, 3098. Becke, A. D. *J. Chem. Phys.* **1993**, *98*, 1372; Becke, A. D. *J. Chem. Phys.* **1993**, *98*, 5648.

(14) Bauschlicher, C. W., Jr.; Partridge, H. *Chem. Phys. Lett.* **1995**, *240*, 533.

(15) Blomberg, M. R. A.; Siegbahn, P. E. M.; Svensson, M. *J. Chem. Phys.* **1996**, *104*, 9546.

(16) Siegbahn, P. E. M.; Crabtree, R. H. *J. Am. Chem. Soc.* **1997**, *119*, 3103.

(17) Shu, L.; Nesheim, J. C.; Kauffmann, K.; Munck, E.; Lipscomb, J. D.; Que, L., Jr. *Science* **1997**, *275*, 515.

(18) Frisch, M. J.; Trucks, G. W.; Schlegel, H. B.; Gill, P. M. W.; Johnson, B. G.; Robb, M. A.; Cheeseman, J. R.; Keith, T.; Petersson, G. A.; Montgomery, J. A.; Raghavachari, K.; Al-Laham, M. A.; Zakrzewski, V. G.; Ortiz, J. V.; Foresman, J. B.; Cioslowski, J.; Stefanov, B. B.; Nanyakkara, A.; Challacombe, M.; Peng, C. Y.; Ayala, P. Y.; Chen, W.; Wong, M. W.; Andres, J. L.; Replogle, E. S.; Gomperts, R.; Martin, R. L.; Fox, D. J.; Binkley, J. S.; Defrees, D. J.; Baker, J.; Stewart, J. P.; Head-Gordon, M.; Gonzalez, C.; Pople, J. A. *Gaussian 94 Revision B.2*; Gaussian Inc.: Pittsburgh, PA, 1995.

(19) Stevens, P. J.; Devlin, F. J.; Chablowski, C. F.; Frisch, M. J. *J. Phys. Chem.* **1994**, *98*, 11623.

(20) Lee, C.; Yang, W.; Parr, R. G. *Phys. Rev.* **1988**, *B37*, 785.

(21) Vosko, S. H.; Wilk, L.; Nusair, M. *Can. J. Phys.* **1980**, *58*, 1200.

coefficients were determined, but used the correlation functionals of Perdew and Wang instead.[22]

The B3LYP energy calculations were made using the large 6-311+G-(2d,2p) basis set in the GAUSSIAN-94 program. This basis set has two sets of polarization functions on all atoms including two f-sets on the metals, and also diffuse functions. In the B3LYP geometry optimizations a much smaller basis set, the LANL2DZ set of the Gaussian-94 program, was used. For the iron and nickel atoms this means that a nonrelativistic ECP according to Hay and Wadt[23] was used. The metal valence basis set used in connection with this ECP is essentially of double-ζ quality. The rest of the atoms are described by standard double-ζ basis sets.

The computational model systems used in the present work are quite large by quantum chemical standards. The calculations could still be successfully performed using very large basis sets and accurate methods, as described above. However, the calculations of accurate Hessians turned out to be prohibitively expensive. Not only are the systems too big, but it was also very difficult to obtain sufficient convergence for obtaining numerically reliable frequencies. After considerable difficulties it was finally possible to obtain Hartree−Fock frequencies for the reactant and transition state complexes. These zero-point energies were scaled by a factor of 0.9 as usual. For the other complexes zero-point vibrational effects had to be estimated on the basis of similar systems. Overall, the relative zero-point effects are quite small, on the order of 1−2 kcal/mol, so the lower accuracy for these effects is not critical.

III. Results and Discussion

To perform a quantum chemical study of an enzymatic reaction, a reasonable knowledge of the active site is absolutely necessary. As mentioned in the Introduction, two recent experiments were particularly important in this respect. First, the X-ray crystal structure of the inactive form of the iron−nickel hydrogenase from *D. gigas* was very important together with the definitive assignment of the second metal as iron.[6b] Second, the identification of the three diatomic ligands on iron as two CN and one CO[8] was the finding that actually triggered the present study. However, there are still many uncertainties concerning the actual structure of the active metal center that remain unresolved. Since hydrogen atoms are not located in the X-ray structure, the most severe of the initial problems was to assign the positions of the hydrogen atoms and thereby the oxidation states of the metals because a neutral cluster model was chosen. More precisely, the character of the four participating cysteine ligands either as the anionic thiolate or neutral thiol forms had to be determined. The design of the present chemical model to be used in the H−H activation therefore constituted a major part of the present study and is described below in subsection a. The results for the H−H activation and the discussion and analysis of the results are covered in subsection b. It is important to note that we cannot expect to account for the effects of the polypeptide matrix on the behavior of the core cluster; this matrix cannot be included in the calculation because of the size and complexity of the polypetide. Nevertheless, the quantum chemical method described here has previously proved successful at modeling important aspects of enzyme behavior, as in the case of the Fe_2 cluster of MMO, where biophysical data supporting the computationally-derived structure of the proposed key intermediate was obtained after the computational study.[16]

a. Chemical Model. The experimentally determined structure of the nickel−iron hydrogenase contains four cysteine ligands. The protonation states of these ligands (Cys^- or CysH) are unknown and therefore have to be determined. The computational procedure is simply to try all possibilities and compare with the available experimental results. The criteria used to decide on the final model is that the structure has to agree reasonably well with the X-ray structure with the important caveat that this structure is for the inactive form of the enzyme, and also that the final energetics for the H−H activation reaction has to agree with what is known for the enzyme. A starting point for this investigation is to consider the nickel−iron complex to be neutral. This is a reasonable assumption since charges are not stabilized in general in the low dielectric medium of a protein.[24,25] To simplify the present study, an SH group is used as a model for the unprotonated cysteine ligand and H_2S is used as the protonated form. This is expected to allow for a sufficiently accurate description of the metal spin states which are critical for the chemistry of the enzyme. While the SH model is expected to lead to reasonable metal−sulfur bond distances, the use of H_2S might lead to slightly too long metal−sulfur distances, but this should have only marginal effects on the energetics.

The first cysteine ligands investigated were the bridging ligands. Choosing these ligands as SH leads to a structure with a reasonable nickel−iron distance of 2.8−3.0 Å depending on the other ligands, and also reproduces the initially surprising bending, found experimentally, of the complex at the bridging groups. Had these ligands been hydroxyl groups a planar Ni−$(OH)_2$−Fe structure might be expected, but with sulfur-containing ligands a strongly bent Ni−$(SH)_2$−Fe structure is found. The bending, which moves the metal atoms closer to each other, is associated with a Fe−S−Ni angle close to 90°. The reason for this structural difference between bridging oxygen-derived and sulfur-derived ligands is that, in the case of oxygen, the mixing of the 2s and 2p orbitals to make sp^2 hybrids is easier, while the bonding orbitals tend to be unhybridized 3p orbitals with 90° bond angles in the case of sulfur.

The second choice for the bridging groups is to use H_2S ligands. If this is done, there is a loss of coordination to one of the metal atoms. This leads to much too long nickel−iron distances of 3.7 Å compared to the experimental distance of 2.9 Å, and also to the wrong bending angle at the bridging cysteines. H_2S ligands can therefore be ruled out as good models for the bridging groups. In other words, protonation of the bridging cysteine ligands in the resting enzyme is ruled out. SH bridging ligands, on the other hand, lead to a good overall agreement with the experimental structure.

Having determined the two bridging ligands to be modeled with SH groups, the next question concerns the terminal cysteine ligands on nickel. There are three possibilities; both cysteines should be modeled with SH groups, both should be modeled with H_2S groups, or there should be one of each. Each assignment implies a different oxidation level for the cluster because of the neutral net charge of the model chosen. Starting with both cysteines as SH groups leads to a triplet ground state for the complex and a formal oxidation level of NiFe(III,III) for the metals in the cluster. The coordination geometry around nickel is planar with equal Ni−S bond distances of about 2.3

(22) Perdew, J. P.; Wang, Y. *Phys. Rev. B* **1992**, *45*, 13244. Perdew, J. P. In *Electronic Structure of Solids*; Ziesche, P., Eischrig, H., Eds.; Akademie Verlag: Berlin, 1991. Perdew, J. P.; Chevary, J. A.; Vosko, S. H.; Jackson, K. A.; Pederson, M. R.; Singh, D. J.; Fiolhais, C. *Phys. Rev. B* **1992**, *46*, 6671.

(23) Hay, P. J.; Wadt, W. R. *J. Chem. Phys.* **1985**, *82*, 299.

(24) See, for example: Lippard, S. J.; Berg, J. M. *Principles of Bioinorganic Chemistry*; University Science Books: 1994.

(25) (a) Rich, P. R. In *Protein Electron Transfer*; Bendall, D. S., Ed.; BIOS Scientific Publishers Ltd.: Oxford, U.K., 1996; pp 217−248. (b) Rich, P. R.; Meuner, B.; Mitchell, R.; Moody, A. J. *Biochim. Biophys. Acta* **1996**, *1275*, 91−95. (c) Moore, G. R.; Pettigrew, G. W.; Rogers, N. K. *Proc. Natl. Acad. Sci. U.S.A.* **1986**, *83*, 4998-4999.

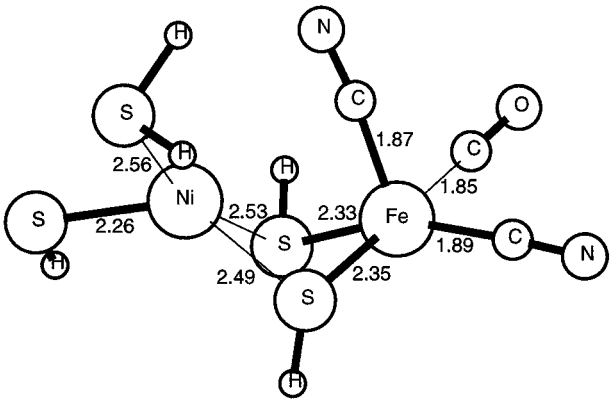

1

Figure 2. Quartet reactant model of nickel−iron hydrogenase **1**. The Ni−Fe distance is 3.03 Å.

Å. Also the Fe−S bond distances are approximately 2.3 Å. This structure could imply a Ni(IV) oxidation state, but this is contradicted by the spin population on nickel which is only −0.1. The spin population on iron is 1.0, and there are also large spins on the terminal SH groups of about 0.5 each. A few key factors indicate that this is not a good model for the real nickel−iron hydrogenase complex. First, the structure determined experimentally does not have a planar geometry around nickel, but a highly distorted square pyramid.[6b] Second, the spins on the terminal SH ligands appear to be too large. When two hydrogen atoms are bound to these ligands, the total binding energy is calculated to be as large as 143 kcal/mol which is much more than the binding energy of H_2 of only 104 kcal/mol. This means that this triplet structure cannot be a good model for nickel−iron hydrogenases since the reaction with H_2 would be far too exothermic. The model with two terminal unprotonated cysteines is therefore ruled out.

Selecting between the two remaining cases, the first with two terminal protonated cysteines and the second with one unprotonated and one protonated cysteine, is much more difficult. In both cases, structures closely resembling the experimental one are obtained. With two protonated cysteines (modeled by H_2S groups) a triplet ground state with a metal oxidation state of NiFe(II,II) is found with a nickel−iron distance of 2.93 Å in good agreement with that of the experimentally determined distance of 2.9 Å. The four metal−sulfur bridge distances are all rather similar in the range 2.41−2.47 Å, which is somewhat different from that of the experimentally found distances of 2.2 Å for iron−sulfur and 2.6 Å for nickel−sulfur distances. With one terminal H_2S and one SH the ground state is a quartet with a metal oxidation state of NiFe(II,III). We write the assignment in this way to avoid assigning particular oxidation states to the individual metals, Fe or Ni, in what is best described as a quite spin-delocalized system. This form has a nickel−iron distance of 3.0 Å (experimental 2.9 Å). The bridge distances are much better for this structure with iron−sulfur distances of about 2.3 Å (experimental 2.2 Å) and nickel−sulfur distances of about 2.5 Å (experimental 2.6 Å); see Figure 2. This agreement is one reason this structure was selected as the model for the H−H activation studies of nickel−iron hydrogenase, but the most important reason is that this is the model that best reproduces the experimental energetics of the entire reaction, as shown in the next subsection.

Before the results of the H_2 activation reaction are discussed in the next subsection, some comments should be made concerning the fate of the protons and electrons produced by the reaction. In an interesting result, Hembre et al.[12c] have shown how Cp*Ru(dppf)H (dppf = 1,1′-bis(diphenylphosphino)ferrocene) can catalyze H_2 reduction of ferricinium ion to ferrocene or MV^{2+} to MV^{+}. Thornley[26] has persuasively argued that, in the case of nitrogenase, the transfer of electrons (ET) and protons (PT) is closely coupled. In a recent paper,[27] we have suggested that, in other cases of what is normally considered electron transfer in proteins, the process is better described as a hydrogen atom transfer (HAT) where the motions of the electron and of an accompanying proton are closely coupled, mediated by hydrogen-bonded chains of residues. Although work in this area is at a very early stage, such chains have been identified in certain proteins. In ribonucleotide reductase (RNR), for example, the structural data show that such a chain is present and site-directed mutagensis shows that this chain is indeed involved in "electron transfer".[28] In what follows we have therefore used the language and ideas of HAT to describe hydrogenase chemistry. The key points of our analysis are not affected if the HAT picture is replaced by a more conventional ET/PT picture, however. The HAT picture is also useful for obtaining the energetics of the redox processes involved. While we believe that HAT is indeed one possibility to describe electron transfer in the hydrogenase system, we defer a full discussion of this aspect to a future paper in order to maintain focus on other aspects of hydrogenase chemistry, notably the H_2 activation step.

b. H−H Activation and Hydrogen Transport. Energies are in general much more critical tests of a model than are the structures. From the structural test described above, the best model of the reactant complex should be the one shown in Figure 2. It has two bridging SH groups and one SH and one H_2S as terminal ligands for nickel. There are three close-lying states of this neutral reactant of which the quartet turns out to be most interesting for the H_2 reaction. The final test this model must survive is that it should reproduce what is known about the energetics of the H_2 reaction. This means that the activation of H_2 should have a barrier of about 10 kcal/mol and be only slightly exothermic. Formation of a molecular precursor is also thought likely. A schematic illustration of the suggested reaction path based on the present results is shown in Scheme 1.

Several attempts were made to find molecular H_2 precursors, but the only site where H_2 was found to bind significantly is the iron. The quartet H_2 complex found is shown in Figure 3. At the highest level of calculation the binding energy is 3.1 kcal/mol for this state. For the reactant there are also low-lying doublet and sextet states. The doublet state is essentially an antiferromagnetically coupled complex corresponding to the ferromagnetically coupled quartet state. As usual for these types of bimetallic complexes, the ferromagnetic and antiferromagnetic states are chemically very similar and lie close in energy. This was also shown for some Mn_2 complexes[29] and for the case of MMO.[16] It is therefore not surprising that the doublet state of the molecular H_2 precursor has an energy quite similar to that of the quartet state. In what follows, this doublet state, which converges only with difficulty, will not be discussed further but will be assumed to behave like the quartet state. For the reactant there is also a sextet state which is chemically quite different and does not form a molecular precursor with

(26) Thornley, R. N. F. In *New Horizons in Nitrogen Fixation*; Palacias, R., Ed.; Kluwer: Dordrecht, The Netherlands, 1993; p 79.

(27) Siegbahn, P. E. M.; Blomberg, M. R. A.; Crabtree, R. H. *Theor. Chem. Acc*., in press.

(28) Ekberg, M.; Sahlin, M.; Eriksson, M.; Sjöberg, B. M. *J. Biol. Chem.* **1996**, *271*, 20655.

(29) Blomberg, M. R. A.; Siegbahn, P. E. M.; Styring, S.; Babcock, G. T.; Åkermark, B.; Korall, P. Submitted to *J. Am. Chem. Soc.*

Scheme 1. A Schematic Illustration of the Reaction Path Suggested on the Basis of the Present Calculations

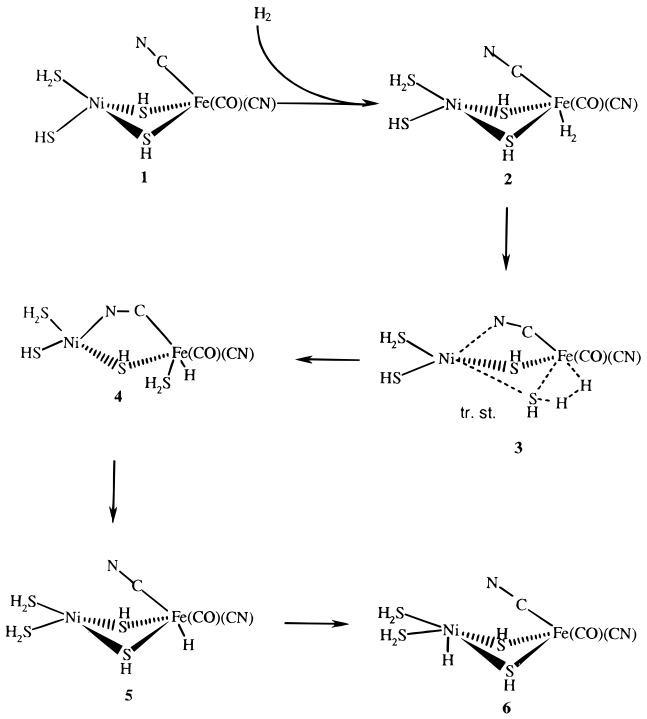

H_2. The finding that lower spin states bind H_2 better than higher ones is rather general and is explained by a greater flexibility for rehybridization of the metal d-shell. In such a rehybridization, the metal partly deshields its positive nucleus which introduces an electrostatic attraction of H_2.[30] The high-spin sextet state is also found to have quite a high barrier for H−H dissociation. It is therefore ruled out as a model for the experimental cluster, and is not discussed further. It should be pointed out that this does not put any additional requirement on the enzyme, since spin state changes are quite rapid, allowing the system facile crossings from one potential energy surface to the other whenever required.

The presence of a molecular H_2 precursor, which has been suggested previously,[31] gives a simple explanation why CO inhibits the H−H activation reaction. Placing CO at the iron site where H_2 should bind leads to quite a large binding energy of 32 kcal/mol for CO. It is clear that a hydrogen molecule which binds by only 3.1 kcal/mol cannot substitute this CO, and the system is therefore poisoned. Dihydrogen binding in the molecular form is known to facilitate subsequent heterolytic cleavage.[32] A number of dihydrogen complexes, especially when bound to weak π-donor sites, are known to behave as proton acids, the experimental pK_a values for isolable species being in the range +15 to −2. This acidity is consistent with the heterolytic splitting of H_2 in which a proton moves to an adjacent basic site and a hydride remains bound to the metal.

The next step of the reaction, where the H−H bond breaks, is the most difficult part to treat computationally. In the present study this part is further complicated by the fact that it is too expensive to calculate accurate Hessian matrices; see section II. The search for the transition state started out from the molecular H_2 precursor and then approached the transition state

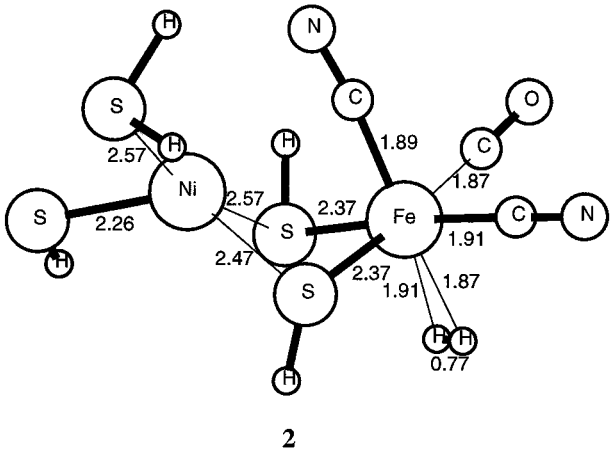

2

Figure 3. Molecular H_2 precursor of nickel−iron hydrogenase **2**. The Ni−Fe distance is 3.05 Å. The energy is 3.1 kcal/mol lower than for the structure in Figure 2 (**1**).

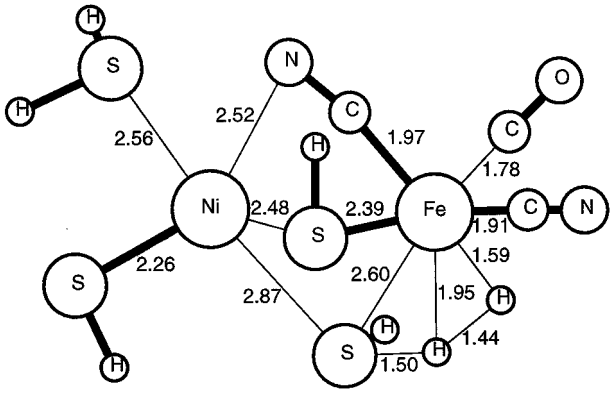

3

Figure 4. Transition state for H_2 dissociation of nickel−iron hydrogenase **3**. The Ni−Fe distance is 3.08 Å. When the SH model is used, the energy is 7.9 kcal/mol higher than for the structure in Figure 2 (**1**). When the hydrogen of SH was replaced with a CH_3 group, a value of 5.6 kcal/mol was obtained.

by freezing the H−H distance at different incremental values, optimizing all other degrees of freedom. In the region of the transition state, an approximate Hessian was obtained at the Hartree−Fock level using a small basis set. The approximate character of the Hessian used in the optimization does not affect the accuracy of the transition state structure obtained, but only affects the convergence pattern to reach this structure. Using this Hessian, a full transition state geometry optimization was performed and the structure shown in Figure 4 was obtained. The structure in Figure 4 indicates a rather complicated heterolytic H−H dissociation mechanism with a hydride binding to iron, as expected, but with the other hydrogen binding as a proton to a bridging cysteinethiolate group. Protonation of a bridging thiolate ligand after the heterolytic cleavage has been suggested before on the basis of EPR experiments on a selenium-containing hydrogenase from *Methanococcus voltae*.[33] As this happens, the protonated Cys dissociates from the nickel. A simultaneous motion brings one of the CN ligands on iron closer to the nickel, with which it bridges in a rare σ, π bridging mode. The Ni−CN distance of 2.52 Å indicates that some binding is present. This effect could be one reason for the presence of the rather unusual CN ligand on iron. The CN and

(30) Siegbahn, P. E. M.; Svensson, M. *J. Am. Chem. Soc.* **1994**, *116*, 10124.

(31) Crabtree, R. H. *Inorg. Chim. Acta* **1986**, *125*, L7.

(32) Lough, A. J.; Park, S.; Ramachandran, R.; Morris, R. H. *J. Am. Chem. Soc.* **1994**, *116*, 8356. Lee, J. C.; Peris, E.; Rheingold, A. L.; Crabtree, R. H. *J. Am. Chem. Soc.* **1994**, *116*, 11014.

(33) Sorgenfrei, O.; Möller, S.; Pfieffer, M.; Sniezko, I.; Klein, A. *Arch. Microbiol.* **1997**, *167*, 189.

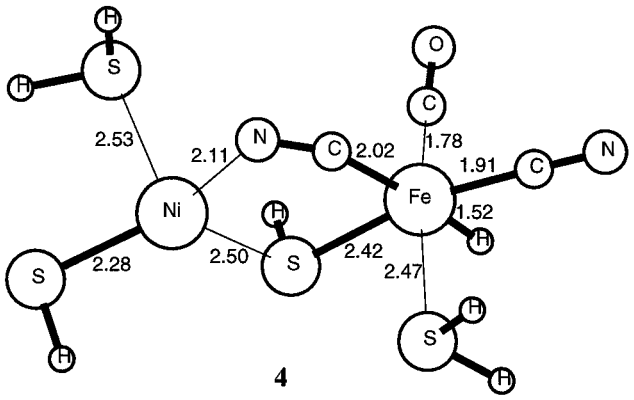

Figure 5. Quartet product structure **4** obtained after H_2 dissociation of nickel−iron hydrogenase **3**. The Ni−Fe distance is 3.74 Å. The energy is 6.6 kcal/mol lower than for the structure in Figure 2 (**1**).

CO ligands also clearly have a reducing effect on the iron spin which should also be quite important. Interaction between one of the CN ligands and nickel has never been reported before for hydrogenases.[34] At the highest level, the barrier height for H−H dissociation is 11.0 kcal/mol with respect to the precursor well. Of course, we cannot definitively exclude the possibility that the proton resides on some other basic group, such as a basic residue in the polypeptide, nor the possibility that the rearrangements observed in the quantum study are inhibited by the polypeptide matrix, which could hydrogen bond to the inner sphere ligands and constrain their motion. Alternatively, the CN and CO ligands may be buried in the polypeptide matrix and steric effects may prevent their transit.

Since it was found that a bridging cysteine ligand is directly involved in the H−H activation, the use of the simple SH model might be questioned. A set of calculations were therefore set up where the hydrogen of SH is replaced by a methyl group. Freezing the H−H distance and optimizing all other degrees of freedom lead to an estimated effect of the methyl substitution on the barrier height of −2.3 kcal/mol. The best predicted barrier height for the real reaction is therefore 11.0 − 2.3 = 8.7 kcal/mol, a value remarkably close to the experimental activation energy of 10 kcal/mol.[35]

Several other H−H dissociation pathways were also studied following the same procedure as described above of stepwise freezing the H−H distance. The most interesting of these is a similar dissociation on the nickel center. At the same level of theory, using the medium-sized LANL2DZ basis set, the dissociation on nickel is found to be about 10 kcal/mol less favorable than that on iron described above. A direct nickel participation in the H−H dissociation is therefore unlikely.

As the H−H transition state is passed on the iron center, the product structure shown in Figure 5 is reached. This is also a quartet state so the entire reaction occurs on this surface without any spin-crossings. From the molecular H_2 precursor the reaction is weakly exothermic by 3.5 kcal/mol, a quite reasonable value. First, the reaction should be exothermic to have a driving force. Second, since under certain other circumstances the reaction can be driven backward to release H_2,[9a] a large exothermicity in the forward reaction is thus unlikely. The quartet product structure in Figure 5 shows a number of characteristic features: One Fe−H bond of 1.52 Å, and only one bridging cysteine group; the other cysteine is protonated and dissociated from the nickel. Instead, a CN ligand is now bridging, with short bond distances of 2.11 Å to nickel and of 2.02 Å to iron. Although rare, this binding mode is known, for example, in $[Cp'_2Mo_2(CO)_4(\mu\text{-}CN)]^-$ ($Cp' = MeC_4H_4$).[36]

The formal oxidation state for all the proposed intermediates in Scheme 1 is NiFe(II,III). This apparent absurdity is the result of the way formal oxidation state is defined[37] for metal complexes, where an M−H hydrogen is always considered as H^- and an SH hydrogen as H^+. If reduction of the cluster is accompanied by protonation either at the thiolate S or at the metal, the formal oxidation state remains unchanged. More useful for the biophysical chemist is the oxidation level (OL), which reflects the number of electrons added to the cluster and ignores the effect of protonation. This we can define as the formal oxidation state that would result from heterolytic fission of each M−H bond in the sense $M-H \rightarrow M^- + H^+$. With this definition, biochemically reasonable oxidation states are obtained for the intermediates of Scheme 1: for example, **1** and **2** have OL = NiFe(II,III), as before, but **4**, **5**, and **6** have OL = NiFe(I,II), reflecting their two-electron reduction relative to **1** and **2**.

In the full mechanism of the nickel−iron hydrogenase enzyme, the protons and electrons of the hydrogens produced by dissociating H_2 should be transported away from the Ni−Fe complex. The most common view is that the electrons will be transported along a chain of iron−sulfur clusters and amino acids, which starts at one of the cysteines at the nickel center; see Figure 6. This transport could be either an electron transfer or a proton-coupled electron transport; see subsection a. In the latter case, the relevant transport energies are those found by binding hydrogens at different places along the transport chain. Within the Ni−Fe cofactor the hydrogen atoms should then move from the iron to the nickel and then continue away from the cluster along the transport chain. At the end of the entire process, both hydrogens should have left the Ni−Fe cofactor to restore the complex in its original active state. As a first step of modeling the hydrogen transfer, the hydrogen ending up on the cysteine ligand is moved all the way to a terminal cysteine ligand on nickel; see Figure 7. This picture is in line with suggestions that at least one of the cysteine ligands on nickel temporarily becomes protonated after the cleavage of H_2.[6b] This step is found to be almost thermoneutral as it indeed must be to be effective, the energy requirement being only 1.4 kcal/mol. After this step the hydrogen atom directly bound to iron can be moved over to nickel, as seen in Figure 8. The cost of 3.1 kcal/mol is also small, but slightly larger than that for moving the first hydrogen atom. The total cost of moving both hydrogens from the iron to the nickel site, with one hydrogen bound to nickel and one bound to a terminal cysteine, is therefore 4.5 kcal/mol. These different calculated energies show that the hydrogens produced by the H_2 reaction diffuse very easily over to the nickel site toward the transport chain containing the iron−sulfur clusters. Preliminary model calculations show that hydrogen atoms are also bound with a very similar energy to these iron−sulfur clusters provided that the irons are assigned low oxidation states. In future studies of the Ni−Fe enzyme, the proton-uncoupled electron transport model will be tested by computing relevant ionization energies of the Ni−Fe complex and electron affinities of the iron−sulfur clusters.

(34) Withdrawn at galley stage.

(35) McTavish, H.; Sayavedra-Soto, L. A.; Arp, D. *J. Biochem. Biophys. Acta* **1996**, *1294*, 183.

(36) Curtis, M. D.; Hau, K. R.; Butler, W. M. *Inorg. Chem.* **1980**, *19*, 2096.

(37) Crabtree, R. H. *The Organometallic Chemistry of the Transition Metals*, 2nd ed.; Wiley: New York, 1994; p 35.

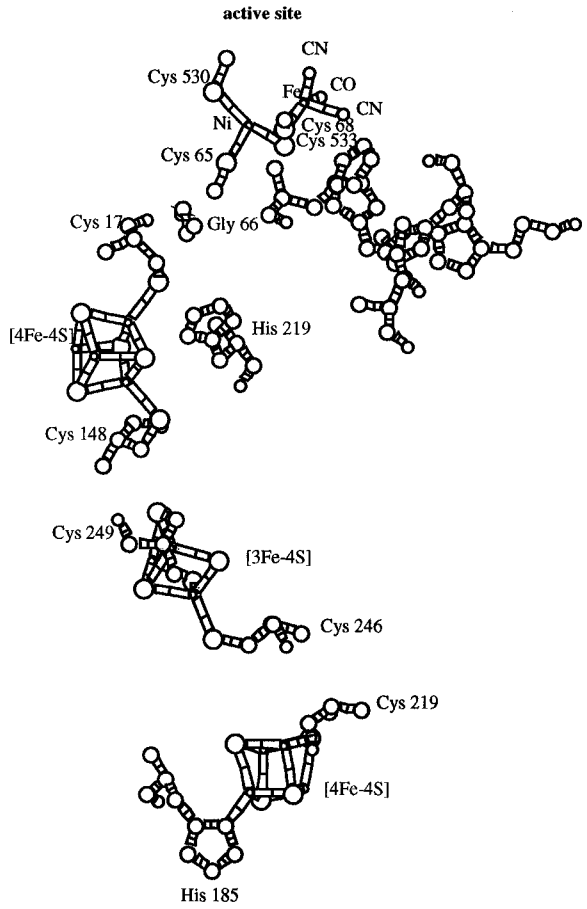

Figure 6. Relative location of the redox-active cofactors and a proposed hydrogen transport chain obtained from the X-ray structure of nickel−iron hydrogenase.[6]

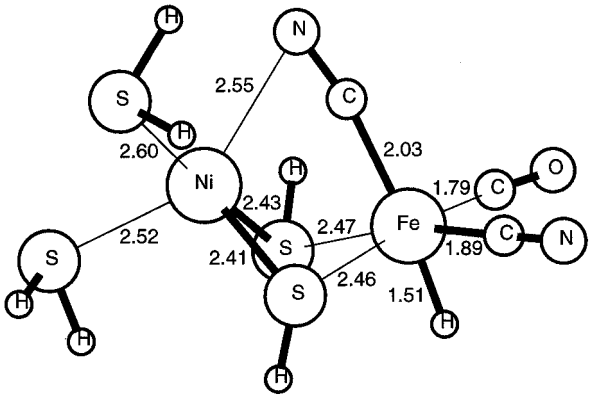

5

Figure 7. Structure where one of the hydrogen atoms produced by the H_2 dissociation has moved to a terminal cysteine ligand on nickel, **5**.

The energetics of the H_2 dissociation reaction are summarized in Table 1 and displayed schematically in Figure 9. The discussion above shows that the energetics obtained using the quartet reactant model with bridging SH groups and terminal SH and H_2S ligands on nickel agree reasonably well with experimental evidence, including a rather low reaction barrier for H−H dissociation and a possibility for easy diffusion of the hydrogen atoms produced by the dissociation. No other model tested agrees as well with experiment as this one.

The second best model tried for the H_2 reaction has two unprotonated cysteines (SH groups) on nickel, rather than only one as in the above model. Since, in this model, H−H activation also occurs on iron with very little influence from nickel, the activation barrier is only modified to a minor extent, compared to the model described above, by the change of ligands on nickel. However, the situation after H−H activation is quite different in the two models. Both unprotonated cysteine ligands on nickel can take up hydrogen. This is a very exothermic step, leading to an overall reaction energy of −42.0 kcal/mol. This model is therefore unrealistic, since the hydrogen atoms produced from the H−H dissociation would then only move to the cysteine ligands on nickel and not move away from the cluster, as they should. The model with two unprotonated cysteine ligands on nickel is therefore ruled out. This model

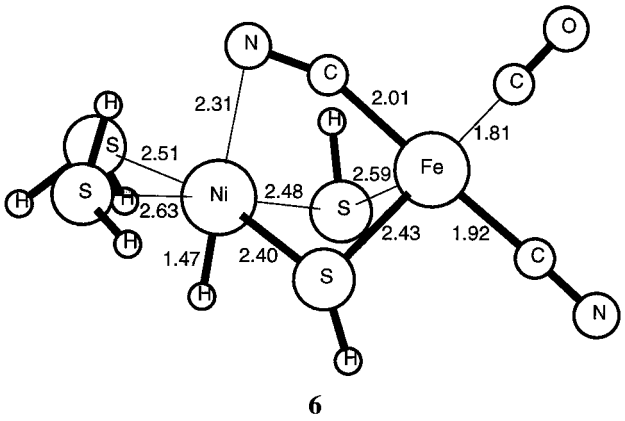

6

Figure 8. Structure where the second hydrogen atom produced by the H_2 dissociation has moved from iron to nickel, **6**.

Table 1. Relative Energies (ΔE) (kcal/mol) and Spin Densities (S) for Points along the Reaction Pathway for H_2 Dissociation on the Quartet Potential Surface (See Also Figure 9)

structure	ΔE	S(Ni)	S(Fe)
SH_2NiSH-$(SH)_2$−$Fe(CN)_2CO$ + H_2 (**1**)	0	1.4	1.0
SH_2NiSH−$(SH)_2$−$Fe(H_2)(CN)_2CO$ (**2**)	−3.1	1.4	0.9
transition state **3**	+7.9[a]	1.4	1.1
SH_2NiSH−$(SH)(CN)$−$FeH(SH_2)(CN)(CO)$ (**4**)	−6.6	1.5	1.1
SH_2NiSH_2−$(SH)_2$−$FeH(CN)_2CO$ (**5**)	−5.2	1.0	2.0
SH_2NiHSH_2−$(SH)_2$−$Fe(CN)_2CO$ (**6**)	−2.1	0.9	2.0

[a] In the case where the hydrogen of SH was replaced with a CH_3 group a value of +5.6 kcal/mol was obtained. See the discussion in subsection III.b.

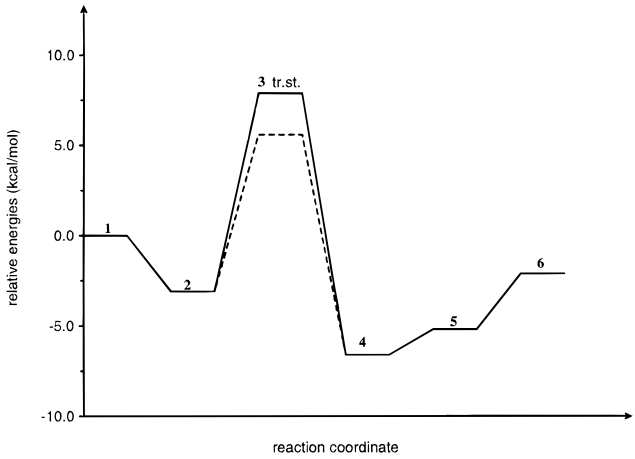

Figure 9. Energetics of the H_2 dissociation reaction on the quartet model of nickel−iron hydrogenase. The dashed line represents the case where the hydrogen of SH was replaced with a CH_3 group (see the discussion in subsection III.b).

also leads to a poorer agreement with the experimentally determined X-ray structures.

The model with two protonated terminal cysteine (H_2S) ligands on nickel gives a reasonable geometry for the reactant structure, as described above. The ground state for this structure is a triplet, and the H−H dissociation is found to proceed on this surface. As for the other models, the best dissociation site is iron. However, at the same level of accuracy, the computed barrier is found to be 21 kcal/mol higher than that of the best quartet model. This also rules out this model of the Ni−Fe complex.

A few additional comments should also be made on the electronic structures of the complexes appearing on the reaction pathway. As seen in Table 1 the spins on iron and nickel change surprisingly little during the reaction. The spin population on nickel of 1.4 is totally unaffected on going from the reactant to the molecular precursor, in passing over the H−H activation transition state, and all the way to the product. This stability is in line with the fact that the Ni X-ray absorption edge shows no shift during the reaction.[11] At the same time the iron spin also stays quite stable in the range 0.9−1.1. As the hydrogen atoms start to move after the reaction, from the iron to the nickel site, the spins on the metals change to a greater extent. When both hydrogen atoms have moved, as in Figure 8, the nickel spin has changed from 1.4 to 0.9 and the iron spin from 1.0 to 2.0. Most of the spin change occurring after the reaction appears because one Fe−H bond is cleaved and one Ni−H bond formed. Apart from the spins on the metals, the spins on the sulfurs can also be quite large, particularly for the SH ligands. For example, in the reactant quartet state, the terminal SH ligand on nickel has a sulfur spin as large as 0.4, while the spins on the bridging SH groups are about 0.1.

Making assignments of the states observed by EPR to structures found in the quantum chemical study cannot be done with great confidence at the present state of the investigation. Nevertheless, we have tried to attack this problem via an investivation of the aerobic inactive form, where a bridging hydroxide rather than a bridging oxo appears to produce optimized structures, and so we have tentatively assumed that the bridging X group is hydroxyl. It should be pointed out that this investigation is only preliminary and not nearly as complete as that of the active enzyme discussed above. On the basis of the results for a few different models, we propose the tentative suggested structure shown in Figure 1 for the aerobic enzyme. Compared to the active quartet reactant discussed above, it has an additional bridging hydroxyl group and also has both terminal nickel cysteine ligands protonated. With these modifications, the complex has the same number of covalent bonds as the active form and is therefore also a quartet state (or, almost equivalently, an antiferromagnetically coupled doublet state; see above). This quartet structure should be visible by EPR and may perhaps be assigned as the inactive Ni-A form of the enzyme. It can only be activated by H_2 over several hours. A likely possibility for this activation process is the following. First, one of the protons of the terminal nickel cysteine ligands interacts with the hydroxyl group to form water. This water molecule will initially bind at the position of the hydroxyl group. The calculated binding energy of water at this position is 8 kcal/mol. As H_2 comes in, the water molecule is dissociated from the complex and the iron side of the complex swings around to form the quartet H_2 molecular precursor structure shown in Figure 3. This structure, with or without H_2, should also be visible by EPR and is assigned as the ready Ni-B form. The EPR silent form, also observed experimentally, should have an additional hydrogen on the terminal nickel cysteine ligand and is in this way able to couple antiferromagnetically to an EPR invisible singlet state. After H−H activation of Ni-B, the structure shown in Figure 5, which is also expected to be visible by EPR, should appear. This structure may possibly be assigned to the Ni-C form. This Ni-C form is sensitive to visible light and changes to another Ni-C′ form upon irradiation. Since this photoreaction shows a strong kinetic isotope effect, a hydrogen atom must move in this reaction. Likely candidates for the Ni-C′ form are therefore the structures shown in Figures 7 and 8, where the hydrogens have moved from the iron to the nickel site. These are only preliminary suggestions, and more work, preferably involving calculations of EPR spectra, are needed to establish these assignments.

IV. Conclusions

In this work, we see that the structure and reactivity pattern on nickel−iron hydrogenases are well reproduced by DFT quantum chemical methods assuming a NiFe(II,III) assignment of the resting cluster oxidation state. The structure and reactivity properties appear to be dependent on the spin states of the cluster, of which several close-lying states were identified. After discarding a number of less satisfactory pathways, one remained, which we propose as our working model for H_2 oxidation by the enzyme. In it, H_2 binds to Fe as a molecular hydrogen complex, and then undergoes heterolytic splitting, with hydride transfer to iron and proton transfer to the adjacent cysteinethiolate ligand. At the same time, the cysteinethiol decoordinates from Ni while remaining bound to iron, and the cyanide on iron binds with the nickel in a rare but known binding fashion. The hydride bound to Fe can then be transferred to Ni which may be a necessary preliminary for subsequent hydrogen atom or electron transport. The transition state for hydrogen splitting was located, and the resulting calculated energy barrier is in remarkably good agreement with the experimental value.

Acknowledgment. We thank Dr. S. P. J. Albracht for generously communicating his data on the identification of the active site ligands in H_2ase. We thank the reviewers for helpful suggestions. R.H.C. thanks the NSF for funding.

JA971681+